Photocatalysis

International Edition: DOI: 10.1002/anie.201507807
German Edition: DOI: 10.1002/ange.201507807

Theoretical Design and Experimental Realization of Quasi Single Electron Enhancement in Plasmonic Catalysis

*Jiale Wang, Tiago V. Alves, Fabiane J. Trindade, Caroline B. de Aquino, Joana C. Pieretti, Sergio H. Domingues, Romulo A. Ando, Fernando R. Ornellas, and Pedro H. C. Camargo**

Abstract: *By a combination of theoretical and experimental design, we probed the effect of a quasi-single electron on the surface plasmon resonance (SPR)-mediated catalytic activities of Ag nanoparticles. Specifically, we started by theoretically investigating how the E-field distribution around the surface of a Ag nanosphere was influenced by static electric field induced by one, two, or three extra fixed electrons embedded in graphene oxide (GO) next to the Ag nanosphere. We found that the presence of the extra electron(s) changed the E-field distributions and led to higher electric field intensities. Then, we experimentally observed that a quasi-single electron trapped at the interface between GO and Ag NPs in Ag NPs supported on graphene oxide (GO-Ag NPs) led to higher catalytic activities as compared to Ag and GO-Ag NPs without electrons trapped at the interface, representing the first observation of catalytic enhancement promoted by a quasi-single electron.*

It has been established that the surface plasmon resonance (SPR) excitation in plasmonic nanostructures can be put to work to enhance and/or mediate catalytic processes, the so-called plasmonic catalysis.[1–4] As the SPR excitation strongly depends on several parameters that define the plasmonic nanostructure, various efforts have been made to manipulate composition, shape, size, and morphology to enable improved optical, sensing and/or catalytic properties.[5–9]

Even though single electron manipulation has received enormous attention in the field of electronics,[10] its effects over plasmonic properties in metallic nanostructures such as gold (Au) and silver (Ag) remain largely unexploited. Interestingly, under proper conditions, it can be predicted that the static electric field (E-field) induced by a single electron should become comparable to the E-field intensities generated as a result of SPR excitation in plasmonic nanoparticles, thus enabling, at least in principle, the further tuning of their optical properties.[1,10,11]

[*] Dr. J. Wang, Dr. T. V. Alves, Dr. F. J. Trindade, Prof. R. A. Ando, Prof. F. R. Ornellas, Prof. P. H. C. Camargo
Departamento de Química Fundamental, Instituto de Química, Universidade de São Paulo
Av. Prof. Lineu Prestes, 748, 05508-000 São Paulo, SP (Brazil)
E-mail: camargo@iq.usp.br

C. B. de Aquino, J. C. Pieretti, Prof. S. H. Domingues
MackGraphe-Graphene and Nanomaterials Research Center
Mackenzie Presbyterian University
Rua da Consolação, 896, 01302-907 São Paulo, SP (Brazil)

Supporting information for this article is available on the WWW under http://dx.doi.org/10.1002/anie.201507807.

Here, we investigate the effect of a single electron on the near-field optical properties of an Ag nanosphere, and how it could be put to work to enhance its SPR-mediated catalytic activities. We started by theoretically investigating how the E-field distribution and intensity in the vicinity of a Ag nanosphere was influenced by static electric field induced by a fixed single electron embedded in graphene oxide (GO) close to its surface. Then, we experimentally probed this effect by using GO decorated with Ag NPs as a proof-of-concept system, in which a quasi-single electron can be trapped at the GO and Ag interface. The influence of the quasi-single electron on the SPR-mediated catalytic activities of Ag NPs supported on GO was studied employing the oxidation of *p*-aminothiophenol (PATP) to *p,p′*-dimercaptoazobenzene (DMAB) as a model reaction. By combining our theoretical modeling and experimental design, it was possible to isolate the effect of a quasi-single electron on the improvement of the SPR-mediated catalytic activities in GO-Ag NPs.[12,13]

In order to theoretically design the influence of a quasi-single electron on the enhancement of SPR-mediated catalytic activities, we started by evaluating how the introduction of an extra electron, fixed very close to the Ag NPs surface, would influence the electric field (E-field) distribution and intensity produced as a result of the SPR excitation employing 632.8 nm as the incoming electromagnetic wave. In plasmonic metal nanoparticles less than 100 nm in diameter, it can be expected that the E-field intensity induced by an extra single electron is comparable to the E-field induced by an incoming laser from commercial Raman spectrometers.[1,10,11] For example, if we consider the E-field magnitude at a 10 nm distance from a single electron, the static electric field induced by the electron is 10 times higher relative to the E-field intensity from the incident light under 0.5 mW power.[3] Therefore, if we wish to introduce a relatively small perturbation on the E-field distribution originated from SPR excitation, a material with a high dielectric constant must be introduced. In this context, graphene oxide (GO) represents a very likely candidate due to its high dielectric constant.[14] Moreover, due to the smaller work function of plasmonic metals such as Ag relative to GO,[15,16] its energy band bends towards smaller energy values enabling the formation of a quantum well that can trap free electrons at the GO and Ag interface in the presence of an insulating layer as depicted in Figure 1 a. On the contrary, if this insulating layer is partially removed by a mild annealing, for example, no electrons should be trapped at the interface (Figure 1 b). Here, Ag NPs 20 nm in diameter were chosen as a model system to theoretically investigate the near-field optical

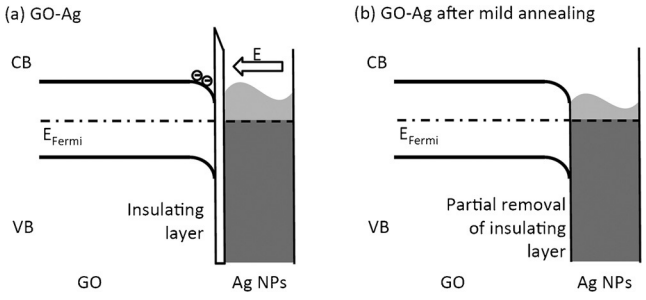

Figure 1. Energy level diagrams for the GO-Ag NPs. a) Extra electrons trapped at the interface due to the presence of an insulating layer provide an additional static electric field that influences the SPR properties of Ag. b) In the absence of an insulating layer extra electrons cannot be trapped at the interface.

properties in the presence of graphene oxide and extra electrons.[17]

It is important to note that the near-field amplitudes in the vicinity of Ag NPs should decrease at 785 nm excitation relative 632.8 nm.[18] Moreover, many Raman probe molecules, such as rhodamine 6G (R6G), PATP, and DMAB, display surface-enhanced resonance Raman scattering (SERRS) effects under 514 nm excitation, which could hamper the experimental verification of our theoretical modeling.[19,20] Consequently, we focused herein in 632.8 nm as the excitation wavelength. The laser power was chosen to be 0.5 mW, in which the effect of a single extra electron should be noticeable under our proposed conditions.

GO represents a complex chemical system consisting of a graphene sheet covalently bound to oxygen-bearing groups, with epoxy and hydroxy functional groups occupying the basal plane.[21,22] Normally, a neat single-layer GO with smooth surface displays a height of 1.45 nm, which is slightly greater than that of a graphene sheet due to the presence of functional groups at the GO surface.[23] As the GO produced by Hummers method normally possesses 2–3 layers,[24,25] we decided to fix the trapped electrons in our simulations at a 2 nm distance from the Ag nanosphere surface and embedded in a GO ultrathin monolayer (so that the volume inside GO can be disregarded).

Figure 2a depicts E-field enhancement contours ($|\mathbf{E}|^2/|\mathbf{E}_0|^2$) around an Ag nanosphere 20 nm in diameter. The maximum E-field enhancement was increased by 4.39 folds relative to the E-field from the incident light ($|\mathbf{E}_{max}|^2/|\mathbf{E}_0|^2$) and was almost symmetrical because of the small size of the nanosphere.[26,27] Figure 2b shows the $|\mathbf{E}|^2/|\mathbf{E}_0|^2$ contours for a 20 nm Ag nanosphere in the presence of a single extra electron, which was fixed at the 12 nm position in the *x*-axis and on 0 nm in *y* (2 nm distance from the Ag nanosphere surface). The electron was embedded in an ultrathin GO monolayer (black dashed line, depicting the GO position). In the presence of a single electron, the E-field contours close to the Ag nanosphere were slightly distorted to the left with $|\mathbf{E}_{max}|^2$ positioned away from the extra single electron as a result of the superposition of the electric field induced by the SPR effect with the static E-field induced by the extra electron. In addition to the distortion on the E-field distribution, the $|\mathbf{E}_{max}|^2/|\mathbf{E}_0|^2$ value increased from 4.39 (without extra electron) to 8.32 (with one extra electron). When two or three extra electrons were added in our calculations (Figure 2c and d, respectively), the E-field distribution close to the particle continued to distort away from the extra electrons and the $|\mathbf{E}_{max}|^2/|\mathbf{E}_0|^2$ values were further increased to 13.71 (Figure 2c, two extra electrons) and 20.58 (Figure 2d, three extra electrons). The E-field enhancement contours by employing the the same $|\mathbf{E}_{max}|^2/|\mathbf{E}_0|^2$ color scale for Ag nanospheres and Ag nanospheres in the presence of one, two, or three electrons is shown in Figure S1 (see the Supporting Information).

Figure S2 and Table S1 summarizes the $|\mathbf{E}_{max}|^2/|\mathbf{E}_0|^2$ values as a function of the Ag nanosphere size without any extra electrons (black trace) and in the presence of 1, 2 or 3 extra electrons (red, blue and magenta traces, respectively) as discussed in Figure 2. For all Ag nanosphere sizes, $|\mathbf{E}_{max}|^2/|\mathbf{E}_0|^2$ increased with the number of extra electrons added in the calculations. Because in experimentally prepared GO decorated with Ag NPs (that we will discuss below) it is expected that Ag NPs will be on both sides of the GO surface, we also performed simulations in which the extra electrons were positioned on the same side with respect to the incident light relative to the position of Ag NPs (Figure S3a–c and Table S1). The obtained E-field distributions were almost the same regardless of the side of the extra electron.

In catalytic applications enhanced and/or mediated by the SPR effect, stronger plasmon oscillations (as manifested by larger $|\mathbf{E}_{max}|^2/|\mathbf{E}_0|^2$) are expected to induce a larger population of electrons that transiently occupy energy states above the Fermi level, which can be subsequently transferred to adsorbed molecules with suitable empty energy levels to trigger transformations involving charge-transfer processes. Stronger plasmon oscillations are also expected to increase local heating during plasmon decay that can provide the energy input for photothermal transformations.[9,28–32] Therefore, according to our simulations, at least in principle, it is possible that the presence of extra electrons can trigger or significantly influence SPR-driven catalytic transformations, even at the single-electron level.

In order to verify this hypothesis, we synthetized GO decorated with Ag NPs (GO-Ag NPs) and designed a series of experiments to probe its SPR-mediated catalytic behavior. The SEM image of the obtained GO-Ag NPs indicated that the Ag NPs had an average diameter of 38 nm, presented a relatively uniform dispersion over the GO material, and were deposited on both sides of its surface (Figure S4). The E-field enhancement contours ($|\mathbf{E}|^2/|\mathbf{E}_0|^2$) calculated around an Ag nanosphere 38 nm in diameter without any extra electrons and in the presence of 1, 2, or 3 extra electrons are depicted in Figure S5a–d. It can be observed that the results were similar to those described when the diameter was 20 nm, and no significant changes over the $|\mathbf{E}_{max}|^2/|\mathbf{E}_0|^2$ values were detected when the electron was considered to be positioned either on the opposite or the same side relative to the incoming electromagnetic wave (Table S1). The Raman spectra of GO-Ag NPs (Figure S6) and the G band position, G/D intensity ratio, and full width at half maximum (Figure S7) did not change as a function of laser power, indicating

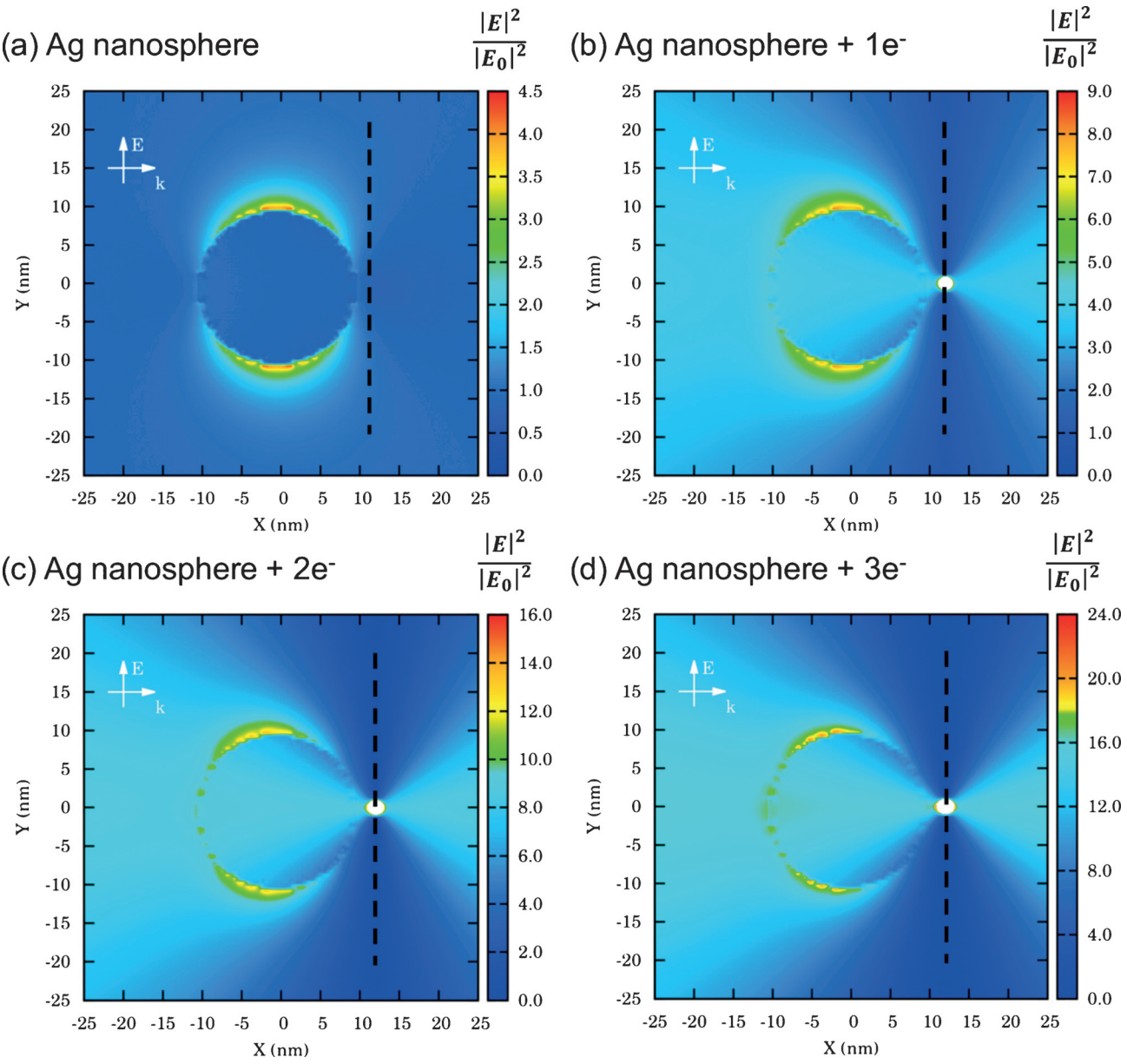

Figure 2. E-field ($|\mathbf{E}|^2/|\mathbf{E}_0|^2$) contours for a Ag nanosphere 20 nm in diameter under 632.8 nm excitation and 0.5 mW as the irradiation power: a) without any extra electrons and with b) one, c) two, and d) three extra electrons positioned on the opposite side relative to the incident light, which was positioned along the [100] direction with polarization on the *y*-axis.

that the partial reduction of GO did not take place under our employed conditions.

In order to experimentally probe the effect of trapped extra electrons on the SPR mediated catalytic activity of GO-Ag NPs as predicted by our simulations, both Ag NPs and GO-Ag NPs were functionalized with PATP, and the SPR-mediated oxidation of PATP to DMAB was investigated. In this case, the selective oxidation of PATP to DMAB is driven by activated O_2 which is generated upon SPR excitation, in which SPR-excited hot electrons from Ag NPs are transferred to adsorbed O_2 molecules from air.[12,13] Figure 3a shows the SERS spectra for Ag NPs (black trace) and GO-Au NPs (red trace) that had been functionalized with PATP molecules employing 0.5 mW as the laser power. The SPR-mediated oxidation of PATP to DMAB could be clearly observed due to the appearance of the bands at assigned to the Ag modes of DMAB.[33,34] The DMAB/PATP + DMAB 1433/1081 cm^{-1} intensity ratios were chosen to probe the PATP to DMAB conversion in Ag and GO-Ag NPs, and the results are presented in Figure 3b. It can be observed that the DMAB/PATP + DMAB 1433/1081 cm^{-1} intensity ratios obtained for GO-Ag NPs (red trace, Figure 3a) was 2.4 fold higher relative to Ag NPs (black trace, Figure 3a).

In order to prove that extra free electrons trapped on the interface between GO and Ag can influence the SPR-mediated catalytic activities, we studied the Raman properties of GO-Ag NPs had been annealed at 120 °C for 45 min before (Figure S8) and after it had been functionalized with PATP

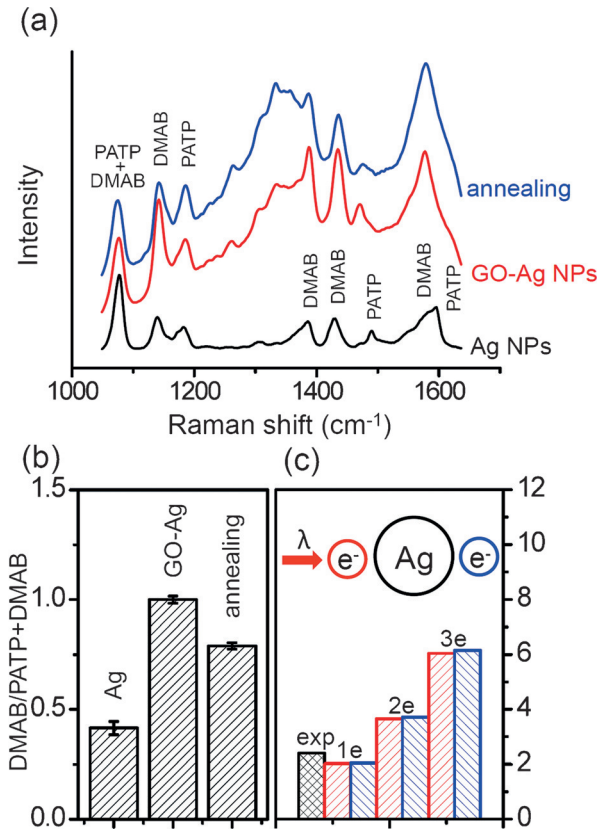

Figure 3. a) SERS spectra for Ag NPs, GO-Ag NPs, and GO-Ag NPs after mild annealing (black, red, and blue traces, respectively) that had been functionalized with PATP employing 0.50 mW as the laser power and 632.8 nm as the excitation wavelength. b) DMAB/PATP + DMAB intensity ratios obtained from (a). c) DMAB/PATP + DMAB intensity ratios for GO-Ag NPs relative to Ag NPs (black squares) and the $|\mathbf{E}_{max}|^2/|\mathbf{E}_0|^2$ values for 1, 2 and 3 electrons trapped at the interface relative to $|\mathbf{E}_{max}|^2/|\mathbf{E}_0|^2$ in the absence of extra electrons. The results with the extra electrons positioned on the same or opposite side of incident light relative to the position of Ag NPs are depicted in red and blue, respectively.

(Figure 3a, blue trace). It is expected that this mild annealing would remove part of the insulating layer between GO and Ag,[35,36] so that electrons should not be able to be trapped at the interface (Figure 1b). As shown in Figure 3a and b, the removal of part of the insulating layer led to a decrease in the DMAB/PATP + DMAB intensity ratios, and this can be related to the absence of extra electrons trapped at the interface as depicted in Figure 1b.

The DMAB/PATP + DMAB 1433/1081 cm^{-1} intensity ratios obtained for GO-Ag relative to Ag NPs at 0.5 mW are also shown in Figure 3c (black bar). The calculated catalytic activity (related to $|\mathbf{E}_{max}|^2/|\mathbf{E}_0|^2$ values) for 1, 2 and 3 extra electrons relative to that without extra electrons as a function of the laser power for Ag NPs 38 nm in diameter are also shown for comparison (the detailed calculations are in the theoretical modeling part in the Supporting Information). In this case, the red and blue bars correspond to the extra electrons positioned at the same and opposite side of the incoming electromagnetic excitation radiation, respectively (as depicted in the inset of Figure 3c). Interestingly, the experimental DMAB/PATP + DMAB 1433/1081 cm^{-1} intensity ratios obtained for GO-Ag NPs relative to Ag NPs were between the calculated catalytic activity ratios for 1 and 2 extra electrons, showing that, at the most, there were two extra electrons trapped in the GO and Ag interface contributing to the detected enhancement in the SPR-mediated catalytic activities.

We also changed the laser power from 0.5 to 0.24 mW and compared the experimental results with the prediction of our theoretical model. At lower laser powers, the effect of the static electric field induced by the presence of extra electrons at the interface should be more significant over the $|\mathbf{E}_{max}|^2/|\mathbf{E}_0|^2$ values. In fact, $|\mathbf{E}_{max}|^2/|\mathbf{E}_0|^2$ calculations under 0.24 mW support this observation, showing that the $|\mathbf{E}_{max}|^2/|\mathbf{E}_0|^2$ values under 0.24 mW laser power were higher than those calculated at 0.5 mW (Table S1 and Figure S9 and S10). Even though the DMAB/PATP + DMAB 1433/1081 cm^{-1} intensity ratios decreased in the samples at 0.24 mW as compared to 0.5 mW, the catalytic activity for the GO-Ag NPs relative to Ag NPs increased by 4.4 folds (Figure S11). If we compare with the calculated catalytic activity related to $|\mathbf{E}_{max}|^2/|\mathbf{E}_0|^2$ results from our simulation (Figure S11c), the observed enhancement ratios were also between the theoretical values involving one and two extra electrons, thus supporting our previous predictions that there was only one single electron, or at most two, trapped at the interface that contributes to the enhancement of SPR-mediated activities. Figure S11a and b also shows the SPR-mediated catalytic investigations of the GO-Ag NPs at 0.24 mW power after annealing at 120 °C for 45 min (blue trace). Similarly to what has been observed with 0.5 mW irradiation, the partial loss of the insulating layer between GO and Ag NPs results in a lower catalytic enhancement relative to Ag NPs due to the lack of extra electrons at the interface.

In summary, we investigated herein the effect of a quasi-single electron on the SPR-mediated catalytic activity of Ag nanoparticles deposited onto GO (GO-Ag NPs). After confirming that the static electric field induced by one, two, or three extra electrons embedded in an ultrathin GO monolayer could significantly change the E-field distribution and intensities around a Ag nanosphere, we employed the SPR-mediated catalytic oxidation of PATP to DMAB as a model reaction to probe the role of extra electrons over the SPR-mediated catalytic activity of Ag in the GO-Ag NPs sample. Our results showed that the SPR-mediated oxidation of PATP to DMAB over GO-Ag NPs in which electrons could be trapped at the GO and Ag interface was increased relative to the individual Ag NPs and the GO-Ag NPs before the partial removal of the insulating layer at the interface, enabling us to isolate the effect of the quasi-single electron trapped at the interface over the activities. We believe that the results presented herein shed new light on the various factors that dictate SPR-mediated catalytic transformations and inspire the rational design of plasmonic processes that can be triggered and/or controlled by single electrons.

Acknowledgements

This work was supported by the Fundação de Amparo à Pesquisa do Estado de Sao Paulo (FAPESP) (grant no. 2013/19861-6) and the Conselho Nacional de Desenvolvimento Cientifíco e Tecnologico (CNPq) (grant no. 471245/2012-7). P.H.C.C., R.A.A., and F.R.O. thank the CNPq for research fellowships. J.W. and T.V.A. thank FAPESP (grant numbers 2013/05709-8 and 2013/07377-2) for fellowships. F.J.T. thanks CNPq (50125/2014-0) for a fellowship. S.H.D., C.B.A. and J.C.P thank FAPESP (SPEC 2012/50259-8) for financial support.

Keywords: graphene oxide · nanoparticles · photocatalysis · silver · surface plasmon resonance

How to cite: *Angew. Chem. Int. Ed.* **2015**, *54*, 14427 – 14431
Angew. Chem. **2015**, *127*, 14635 – 14639

[1] G. Baffoua, R. Quidant, *Chem. Soc. Rev.* **2014**, *43*, 3898 – 3907.
[2] S. Sarina, H. Y. Zhu, E. Jaatinen, Q. Xiao, H. W. Liu, J. F. Jia, C. Chen, J. Zhao, *J. Am. Chem. Soc.* **2013**, *135*, 5793 – 5801.
[3] M. J. Kale, T. Avanesian, P. Christopher, *ACS Catal.* **2014**, *4*, 116 – 128.
[4] J. L. Wang, R. A. Ando, P. H. C. Camargo, *Angew. Chem. Int. Ed.* **2015**, *54*, 6909 – 6912; *Angew. Chem.* **2015**, *127*, 7013 – 7016.
[5] M. A. El-Sayed, *Acc. Chem. Res.* **2001**, *34*, 257 – 264.
[6] C. Burda, X. Chen, R. Narayanan, M. A. El-Sayed, *Chem. Rev.* **2005**, *105*, 1025 – 1102.
[7] Y. Xia, Y. Xiong, B. Lim, S. E. Skrabalak, *Angew. Chem. Int. Ed.* **2009**, *48*, 60 – 103; *Angew. Chem.* **2009**, *121*, 62 – 108.
[8] M. Rycenga, C. M. Cobley, J. Zeng, W. Y. Li, C. H. Moran, Q. Zhang, D. Qin, Y. Xia, *Chem. Rev.* **2011**, *111*, 3669 – 3712.
[9] S. Linic, P. Christopher, D. B. Ingram, *Nat. Mater.* **2011**, *10*, 911 – 921.
[10] L. J. Guo, E. Leobandung, S. Y. Chou, *Science* **1997**, *275*, 649 – 651.
[11] S. Weinberg, *Lectures on Quantum Mechanics*, Cambridge University Press, New York, **2013**.
[12] J. L. Wang, R. A. Ando, P. H. C. Camargo, *ACS Catal.* **2014**, *4*, 3815 – 3819.
[13] Y.-F. Huang, M. Zhang, L.-B. Zhao, J.-M. Feng, D.-Y. Wu, B. Ren, Z. Q. Tian, *Angew. Chem. Int. Ed.* **2014**, *53*, 2353 – 2357; *Angew. Chem.* **2014**, *126*, 2385 – 2389.
[14] M. González-Béjar, K. Peters, G. L. Hallett-Tapley, M. Grenierb, J. C. Scaiano, *Chem. Commun.* **2013**, *49*, 1732 – 1734.
[15] A. Misra, H. Kalita, A. Kottantharayi, *ACS Appl. Mater. Interfaces* **2014**, *6*, 786 – 794.
[16] D. Yang, L. Y. Zhou, L. C. Chen, B. Zhao, J. Zhang, C. Li, *Chem. Commun.* **2012**, *48*, 8078 – 8080.
[17] W. W. Zhang, L. Q. Huang, J. Zhu, Y. Liu, J. Wang, *Mater. Chem. Phys.* **2011**, *131*, 136 – 141.
[18] W. Hermoso, T. V. Alves, F. R. Ornellas, P. H. C. Camargo, *Eur. Phys. J. D* **2012**, *66*, 135.
[19] P. Hildebrandt, M. Stockburger, *J. Phys. Chem.* **1984**, *88*, 5935 – 5944.
[20] A. C. Power, A. J. Betts, J. F. Cassidy, *Analyst* **2011**, *136*, 2794 – 2801.
[21] W. Gao, L. Alemany, L. Ci, P. Ajayan, *Nat. Chem.* **2009**, *1*, 403 – 408.
[22] A. Mathkar, D. Tozier, P. Cox, P. Ong, C. Galande, K. Balakrishnan, A. L. M. Reddy, P. M. Ajayan, *J. Phys. Chem. Lett.* **2012**, *3*, 986 – 991.
[23] I. V. Lightcap, T. H. Kosel, P. V. Kamat, *Nano Lett.* **2010**, *10*, 577 – 583.
[24] S. Stankovich, R. D. Piner, S. T. Nguyen, R. S. Ruoff, *Carbon* **2006**, *44*, 3342 – 3347.
[25] I. N. Kholmanov, S. H. Domingues, H. Chou, X. H. Wang, C. Tan, J.-Y. Kim, H. F. Li, R. Piner, A. J. G. Zarbin, R. S. Ruoff, *ACS Nano* **2013**, *7*, 1811 – 1816.
[26] K. L. Kelly, E. Coronado, L. L. Zhao, G. C. Schatz, *J. Phys. Chem. B* **2003**, *107*, 668 – 677.
[27] E. Hao, G. C. Schatz, *J. Chem. Phys.* **2004**, *120*, 357 – 366.
[28] S. Navalon, M. de Miguel, R. Martin, M. Alvaro, H. Garcia, *J. Am. Chem. Soc.* **2011**, *133*, 2218 – 2226.
[29] P. Christopher, H. Xin, S. Linic, *Nat. Chem.* **2011**, *3*, 467 – 472.
[30] D. N. Denzler, C. Frischkorn, C. Hess, M. Wolf, G. Ertl, *Phys. Rev. Lett.* **2003**, *91*, 226102.
[31] D. G. Busch, W. Ho, *Phys. Rev. Lett.* **1996**, *77*, 1338 – 1341.
[32] M. Bonn, S. Funk, Ch. Hess, D. N. Denzler, C. Stampfl, M. Scheffler, M. Wolf, G. Ertl, *Science* **1999**, *285*, 1042 – 1045.
[33] Y. R. Fang, Y. Z. Li, H. X. Xu, M. T. Sun, *Langmuir* **2010**, *26*, 7737 – 7746.
[34] M. T. Sun, H. X. Xu, *Small* **2012**, *8*, 2777 – 2786.
[35] R. S. Kajen, N. Chandrasekhar, K. L. Pey, C. Vijila, M. Jaiswal, S. Saravanan, A. M. H. Ng, C. P. Wong, K. P. Loh, *ECS Solid State Lett.* **2013**, *2*, M17 – M19.
[36] X. C. Li, B. K. Tay, J. S. Li, D. L. Tan, C. W. Tan, K. Liang, *Nanoscale Res. Lett.* **2012**, *7*, 205.

Received: August 20, 2015
Published online: October 2, 2015

